

Spatial distribution of atoms in the field of the criss-cross standing bichromatic light waves

V. I. Romanenko

Institute of Physics, Nat. Acad. of Sci. of Ukraine (46, Nauky Ave., Kyiv 03680, Ukraine)

N. V. Kornilovska

Kherson National Technical University (24, Berislauske shosse, Kherson 73008, Ukraine)

O. G. Udovytska and L. P. Yatsenko

Institute of Physics, Nat. Acad. of Sci. of Ukraine (46, Nauky Ave., Kyiv 03680, Ukraine)

Abstract

We show that properly detuning the carrier frequency of each of the criss-cross bichromatic waves from the transition frequency in the atom, it is possible to form a two-dimensional trap for atoms if the intensity of the waves is sufficiently large. For zero and near zero initial phases of waves, and also for π and near π phase shift between criss-cross waves a dynamic spatial structure of square cells with the side $\lambda/\sqrt{2}$ is formed. Numerical simulations are carried out for sodium atoms.

PACS numbers: 37.10.Gh, 37.10.Mn, 37.10.Pq

Keywords: optical trap for atoms, standing waves, Monte Carlo wave function method

CONTENTS

I. Introduction	2
II. Interaction of the atom with the field	3
III. The main equations	4
IV. Modelling of the state vector by Monte Carlo wave function method	6
V. Numerical calculation routine	8
VI. Results of the numerical simulation	9
VII. Conclusions	15
Acknowledgments	15
References	15

I. INTRODUCTION

Various aspects of the interaction of atoms with bichromatic standing waves (a pair of monochromatic standing waves with different frequencies), which can also be considered as counter-propagating bichromatic waves or counter-propagating amplitude-modulated waves, have been studied already for three decades. The physical basis of the interaction of atoms with bichromatic waves and numerous experimental work are analyzed, in particular, in the books [1, 2], and in the recent review [3]. The fact that the light pressure force on the atom in the field of a standing bichromatic wave can significantly exceed the force of light pressure in the field of a travelling monochromatic wave [4–9] is essential for the efficient manipulation of atomic beams [9–11]. The field of bichromatic waves, as it turned out, can be used to cool atoms and molecules without the participation of spontaneous emission [12, 13]. This new phenomenon, predicted in [14], will probably enlarge our potential of controlling the motion of molecules by the laser radiation. Another direction of research concerns the formation of traps for atoms only by laser radiation, without additional fields (for example, magnetic field in magneto-trap [1]). The first proposition of such traps was based on the interaction of atoms with the sequences of the counter-propagating light pulses [15–18], then it turned out that the traps can be formed counter-propagating bichromatic [19], stochastic [20] and frequency-modulated [21] waves. In addition, the laser field that confines atoms in the trap can also cool them.

We have considered the interaction of two-level atoms with two orthogonal linearly polarized standing bichromatic waves and found the conditions, for which these waves form a two-dimensional trap for atoms (one-dimensional trap was analyzed in [19]). We have also found the shape and parameters of a grating of atoms, which is formed as a result of their interaction with the field. To describe the motion of atoms in the field, we use the Newton's laws, and the evolution of atomic states we describe by the Monte Carlo wave-function method [22]. Numerical simulation is carried out for sodium atoms.

The paper is organized as follows. In the next section we describe the interaction of the atom with the field, the third section provides the basic equations, the fourth section briefly describes the Monte Carlo wave function method, in the fifth section we explain the procedure of numerical calculation, the obtained results and their discussion are given in the sixth section, short conclusions are formulated at the end of the paper.

II. INTERACTION OF THE ATOM WITH THE FIELD

We consider the atom moving in the field of two criss-cross bichromatic standing waves, each of which is formed by pairs of collinear standing waves. In turn, each of these standing waves can be considered as two counter-propagating monochromatic waves, as shown in Fig. 1.

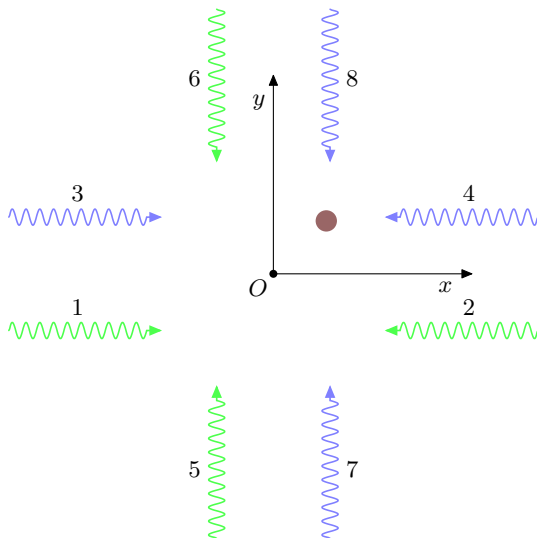


FIG. 1. Schematic interaction of the atom with the field. At the point O the phase difference between the opposite waves is zero. Atom is marked with a circle.

We consider the interaction of atoms with the bichromatic field of standing waves near the point O , where the wave antinodes coincide, that is, the difference between the phases of counter-propagating waves here is zero. In the field of one bichromatic wave, a slight deviation from this point leads to the light pressure force acting on the atom. This force is proportional to the sinus of the phase difference between the standing monochromatic waves that form the standing bichromatic wave [4, 23]. Since this phase difference linearly depends on the coordinates of the atom, a bichromatic standing light wave can form a one-dimensional trap for atoms [6, 19]. Obviously, one can expect that the field of two criss-cross bichromatic waves can form a two-dimensional trap for atoms.

We should note that the interaction of an atom with two criss-cross standing bichromatic waves qualitatively differs from the interaction with one wave. In addition to the absorption of a photon from one travelling bichromatic wave with the following emission of a photon into the oncoming travelling bichromatic wave, there may be the absorption of a photon from one travelling bichromatic wave with subsequent emission of a photon into the orthogonal travelling bichromatic wave. Thus, the result of the atom's interaction with the field of two

standing bichromatic waves can not be considered as the sum of the atomic interactions with each of the standing bichromatic waves.

III. THE MAIN EQUATIONS

The interaction of an atom with a field of criss-cross bichromatic waves can be considered as its interaction with the field of eight travelling monochromatic waves, as shown in Fig. 1. Spatial and time dependence of the field strength of each of them can be described by the equations

$$\mathbf{E}_{n=1,2,3,4} = \mathbf{e}E_{0n} \cos(i\omega_n t \mp ik_n x + i\varphi_n), \quad (1)$$

$$\mathbf{E}_{n=5,6,7,8} = \mathbf{e}E_{0n} \cos(i\omega_n t \mp ik_n y + i\varphi_n), \quad (2)$$

where the sign “ $-$ ” corresponds to an odd n , “ $+$ ” corresponds to an even n , \mathbf{e} is the unit polarization vector, ω_n is the frequency of n -th monochromatic wave. Note that we chose the same direction of the polarization vectors of all the waves. The condition of forming four standing waves by these eight travelling waves is

$$\omega_{2n} = \omega_{2n-1}, \quad n = 1, 2, 3, 4. \quad (3)$$

For the sake of simplicity we consider the standing waves with equal amplitudes,

$$E_{0n} = E_0, \quad n = 1, \dots, 8. \quad (4)$$

We define the detunings δ_n of the frequencies ω_n from the atomic transition frequency ω_0 as

$$\delta_n = \omega_0 - \omega_n, \quad n = 1, \dots, 8, \quad (5)$$

as far as the frequencies of opposing monochromatic waves that form each of the four standing waves are the same (3). We assume that the frequency difference between the monochromatic standing waves that form the bichromatic standing waves, are also the same for both of them:

$$\omega_1 - \omega_3 = \omega_5 - \omega_7 = \Omega > 0. \quad (6)$$

For further simplification, we assume equal mean frequencies of the criss-cross waves, i.e.

$$\frac{\omega_3 + \omega_1}{2} = \frac{\omega_7 + \omega_5}{2} = \omega. \quad (7)$$

From these equations, it is easy to express the frequencies of all monochromatic waves through the mean frequency ω and the frequency difference Ω of the waves:

$$\omega_1 = \omega_5 = \omega + \frac{\Omega}{2}, \quad \omega_3 = \omega_7 = \omega - \frac{\Omega}{2}. \quad (8)$$

Introducing the detuning

$$\delta = \omega_0 - \omega \quad (9)$$

of the mean frequency of bichromatic waves from the transition frequency of the atom and, taking into account (8) and (5), we obtain:

$$\delta_1 = \delta_5 = \delta - \frac{\Omega}{2}, \quad \delta_3 = \delta_7 = \delta + \frac{\Omega}{2}. \quad (10)$$

The field of eight travelling monochromatic waves can be written as a field of four standing waves, the field strength of which has the form

$$\mathbf{E}_{12} = \mathbf{E}_1 + \mathbf{E}_2 = 2E_0\mathbf{e} \cos \left[\omega_1 t + \frac{1}{2}(\varphi_1 + \varphi_2) \right] \cos \left[k_1 x + \frac{1}{2}(\varphi_2 - \varphi_1) \right], \quad (11)$$

$$\mathbf{E}_{34} = \mathbf{E}_3 + \mathbf{E}_4 = 2E_0\mathbf{e} \cos \left[\omega_3 t + \frac{1}{2}(\varphi_3 + \varphi_4) \right] \cos \left[k_3 x + \frac{1}{2}(\varphi_4 - \varphi_3) \right], \quad (12)$$

$$\mathbf{E}_{56} = \mathbf{E}_5 + \mathbf{E}_6 = 2E_0\mathbf{e} \cos \left[\omega_1 t + \frac{1}{2}(\varphi_5 + \varphi_6) \right] \cos \left[k_1 y + \frac{1}{2}(\varphi_6 - \varphi_5) \right], \quad (13)$$

$$\mathbf{E}_{78} = \mathbf{E}_3 + \mathbf{E}_4 = 2E_0\mathbf{e} \cos \left[\omega_3 t + \frac{1}{2}(\varphi_7 + \varphi_8) \right] \cos \left[k_3 y + \frac{1}{2}(\varphi_8 - \varphi_7) \right], \quad (14)$$

and the total field acting on the atom can be written as

$$\mathbf{E} = \mathbf{E}_{12} + \mathbf{E}_{34} + \mathbf{E}_{56} + \mathbf{E}_{78}. \quad (15)$$

Since the first studies of the mechanical action of the bichromatic waves on atoms [4, 6], to calculate the light pressure on atoms the representation of the field in the form of a superposition of the counter-propagating amplitude-modulated waves is also used. This makes it possible to draw an analogy between the field of the bichromatic waves and the field of the sequence of counter-propagating light pulses. This analogy helps to understand why the light pressure force in the field of the bichromatic waves significantly exceeds the light pressure force on an atom in a single travelling wave [24]. In the case of two criss-cross standing waves these counter-propagating waves read

$$\mathbf{E}_{13} = \mathbf{E}_1 + \mathbf{E}_3 = 2E_0\mathbf{e} \cos \left[\omega t - kx + \frac{1}{2}(\varphi_1 + \varphi_3) \right] \cos \left[\frac{1}{2}\Omega t - \frac{1}{2}\Delta kx + \frac{1}{2}(\varphi_3 - \varphi_1) \right], \quad (16)$$

$$\mathbf{E}_{24} = \mathbf{E}_2 + \mathbf{E}_4 = 2E_0\mathbf{e} \cos \left[\omega t + kx + \frac{1}{2}(\varphi_2 + \varphi_4) \right] \cos \left[\frac{1}{2}\Omega t + \frac{1}{2}\Delta kx + \frac{1}{2}(\varphi_4 - \varphi_2) \right], \quad (17)$$

$$\mathbf{E}_{57} = \mathbf{E}_1 + \mathbf{E}_3 = 2E_0\mathbf{e} \cos \left[\omega t - ky + \frac{1}{2}(\varphi_5 + \varphi_7) \right] \cos \left[\frac{1}{2}\Omega t - \frac{1}{2}\Delta ky + \frac{1}{2}(\varphi_7 - \varphi_5) \right], \quad (18)$$

$$\mathbf{E}_{68} = \mathbf{E}_2 + \mathbf{E}_4 = 2E_0\mathbf{e} \cos \left[\omega t + ky + \frac{1}{2}(\varphi_6 + \varphi_8) \right] \cos \left[\frac{1}{2}\Omega t + \frac{1}{2}\Delta ky + \frac{1}{2}(\varphi_8 - \varphi_6) \right], \quad (19)$$

where

$$k = \frac{1}{2}(k_1 + k_3) = \frac{1}{2}(k_2 + k_4), \quad (20)$$

$$\Delta k = k_3 - k_1 = k_4 - k_2 = \Omega/c. \quad (21)$$

The change of the initial time or the reference frame (x and y) is obviously equivalent to the change of initial phases φ_n ($n = 1, \dots, 8$). Since $\Omega \ll \omega$ and $\Delta k \ll k$ changing the initial time, one can make two initial phases equal to zero, and changing the origin of the reference frame one can make four initial phases equal to zero (or their linear combinations).

Projections of the force \mathbf{F} acting on the atom on Ox and Oy axes are [1, 25]

$$F_x = (\varrho_{12}\mathbf{d}_{21} + \varrho_{21}\mathbf{d}_{12}) \frac{\partial \mathbf{E}}{\partial x}, \quad (22)$$

$$F_y = (\varrho_{12}\mathbf{d}_{21} + \varrho_{21}\mathbf{d}_{12}) \frac{\partial \mathbf{E}}{\partial y}, \quad (23)$$

where \mathbf{d}_{ij} ($i, j = 1, 2$) are the matrix elements of the dipole moment, ϱ_{ij} are the elements of the density matrix ϱ . The motion of an atom under the action of this force is described by the second Newton's law

$$\ddot{\mathbf{r}} = \mathbf{F}/m, \quad (24)$$

where m is the mass of the atom, \mathbf{r} is the radius vector of the atom with coordinates x and y .

We find the density matrix using the probability amplitudes c_1 , c_2 of the occupation of the ground $|1\rangle$ and excited $|2\rangle$ states by the atom:

$$\rho_{12} = c_1 c_2^* e^{i\omega_0 t}, \quad \rho_{21} = c_2 c_1^* e^{-i\omega_0 t}. \quad (25)$$

The state vector

$$|\psi\rangle = c_1 |1\rangle + c_2 e^{-i\omega_0 t} |2\rangle, \quad (26)$$

of the atom is calculated from the Schrödinger equation

$$i\hbar \frac{d}{dt} |\psi\rangle = H |\psi\rangle. \quad (27)$$

by modeling the state vector using the Monte Carlo wave-function method [22], which takes into account the possibility of spontaneous emission of light by the atom. Contrary to computations based on the density matrix, this method of calculation allows us to simulate the trajectory of the motion of a single atom.

IV. MODELLING OF THE STATE VECTOR BY MONTE CARLO WAVE FUNCTION METHOD

The Monte Carlo wave-function method for modeling of the state vector [22] provides the numerical solution of the Schrödinger equation (27) with the possibility of spontaneous emission of light by an atom. The spontaneous emission is taken into account by the relaxation term

$$H_{rel} = -\frac{i\hbar}{2} \gamma |2\rangle\langle 2|, \quad (28)$$

where γ is the spontaneous emission rate, in Hamiltonian

$$H = H_0 + H_{int} + H_{rel}. \quad (29)$$

Here

$$H_0 = \hbar\omega_0 |2\rangle\langle 2| \quad (30)$$

describes an atom in the absence of a field and relaxation, and the term

$$H_{int} = -\mathbf{d}_{12}|1\rangle\langle 2|\mathbf{E}(t) - \mathbf{d}_{21}|2\rangle\langle 1|\mathbf{E}(t) \quad (31)$$

is responsible for the interaction of the atom with the field.

Since the Hamiltonian (29) is not Hermitian, we normalize the state vector (26) after each small step in time. The value of the deviation of the vector norm from the unit is used in this case to simulate the process of spontaneous photon emission. With the increase of the deviation, the probability of spontaneous emission increases. The spontaneous emission leads to a quantum jump from an excited state $|2\rangle$ into the ground state $|1\rangle$. Here we use the Monte Carlo wave-function method of the first order of accuracy, described in [22]. Methods of the second and fourth order accuracy are considered in [26].

Let the atom at the time t be described by the state vector $|\psi(t)\rangle$. We find the state vector $|\psi(t + \Delta t)\rangle$ at the time $t + \Delta t$ in two steps.

1. Integrating Schrödinger equation (27) we find the state vector after a sufficiently small Δt :

$$|\psi^{(1)}(t + \Delta t)\rangle = \left(1 - \frac{i\Delta t}{\hbar}H\right)|\psi(t)\rangle. \quad (32)$$

After this step in time, the norm of the state vector equals

$$\langle\psi^{(1)}(t + \Delta t)|\psi^{(1)}(t + \Delta t)\rangle = 1 - \Delta P, \quad (33)$$

where

$$\Delta P = \frac{i\Delta t}{\hbar}\langle\psi(t)|H - H^\dagger|\psi(t)\rangle = \gamma|\Delta t|c_2|^2. \quad (34)$$

2. At the second step, we check whether there was a quantum jump (which accompanies spontaneous emission) during the integration time Δt . For this purpose we compare the value of the random variable ϵ , which is uniformly distributed between zero and one, with ΔP . If $\epsilon < \Delta P$, the quantum jump occurs, the atom passes into the state $|1\rangle$ and the state vector becomes

$$|\psi(t + \Delta t)\rangle = |1\rangle, \quad \epsilon < \Delta P. \quad (35)$$

If $\epsilon > \Delta P$ (in most cases, since $\Delta P \ll 1$), the jump does not occur and state vector (32) obtained at the first stage is normalized:

$$|\psi(t + \Delta t)\rangle = \frac{|\psi^{(1)}(t + \Delta t)\rangle}{\sqrt{1 - \Delta P}}, \quad \Delta P < \epsilon. \quad (36)$$

The direction of propagation of a photon after spontaneous emission we also simulate by the Monte Carlo method, assuming that the propagation directions along the axes Ox and Oy are equally probable (details are given in the fifth section).

Although equation (32) gives a formal solution to the Schrödinger equation, it is more convenient to use the equations for the probability amplitudes c_1, c_2 of populations of states $|1\rangle$ and $|2\rangle$, and, having found them, get the state vector (26). The equations for the amplitudes follow from the Schrödinger equation (27) and are equivalent to it.

Substitution of (26), (29) in (27) gives

$$i\hbar\frac{d}{dt}c_1 = -\mathbf{d}_{12}\mathbf{E}c_2e^{-i\omega_0t}, \quad (37)$$

$$i\hbar\frac{d}{dt}c_2 = -\mathbf{d}_{21}\mathbf{E}c_1e^{i\omega_0t} - \frac{1}{2}\gamma c_2. \quad (38)$$

In the rotating wave approximation (neglecting the exponential terms $\sim e^{\pm 2i\omega_0t}$) [27] from the equations (37), (38) and taking into account

$$\mathbf{E} = \sum_{n=1}^8 \mathbf{E}_n \quad (39)$$

we get

$$\frac{d}{dt}c_1 = -\frac{i}{2}\Omega_0 \sum_{n=1}^4 e^{(-1)^n ik_n x - i\delta_n t + i\varphi_n} c_2 - \frac{i}{2}\Omega_0 \sum_{n=5}^8 e^{(-1)^n ik_n y - i\delta_n t + i\varphi_n} c_2, \quad (40)$$

$$\frac{d}{dt}c_2 = -\frac{i}{2}\Omega_0^* \sum_{n=1}^4 e^{(-1)^{n+1} ik_n x + i\delta_n t - i\varphi_n} c_1 - \frac{i}{2}\Omega_0^* \sum_{n=5}^8 e^{(-1)^{n+1} ik_n y + i\delta_n t - i\varphi_n} c_1 - \frac{1}{2}\gamma c_2, \quad (41)$$

where the Rabi frequency of the monochromatic waves

$$\Omega_0 = -\mathbf{d}_{12}\mathbf{e}E_0/\hbar, \quad (42)$$

is introduced, which, without loss of the generality, we consider to be real [27].

Knowing the probability amplitudes of c_1 , c_2 , one can calculate the light pressure force acting on the atom using (22), (23) and (25). After the averaging of the expressions for the force (22), (23) over time in an interval much greater than the time of fast oscillations with the characteristic time $2\pi/\omega_0$ and at the same time, small enough that the average light pressure force practically does not depend on the time of averaging, we find

$$F_x = \hbar \sum_{n=1}^4 (-1)^{n+1} k_n \operatorname{Im} [c_1 c_2^* \Omega_n^* e^{i\delta_n t - i\varphi_n} e^{i(-1)^{n+1} k_n x}] (|c_1|^2 + |c_2|^2)^{-1}. \quad (43)$$

$$F_y = \hbar \sum_{n=5}^8 (-1)^{n+1} k_n \operatorname{Im} [c_1 c_2^* \Omega_n^* e^{i\delta_n t - i\varphi_n} e^{i(-1)^{n+1} k_n y}] (|c_1|^2 + |c_2|^2)^{-1}. \quad (44)$$

Now we can describe the motion of an atom by integrating simultaneously the equation (24), (40), (41) and taking into account the expressions (43), (44) for the projections F_x , F_y of the light pressure force on the abscissa and ordinate axes.

The normalization in (43), (44) is required for combining integration of the Schrödinger equation and equations of motion by the fourth method order accuracy with the Monte Carlo wave function method of the first order because the intermediate time points are used.

V. NUMERICAL CALCULATION ROUTINE

To simulate the motion of an atom, we simultaneously solve the Newton equation (24) with the force (43), (44) and the equations (40), (41) for the amplitudes of the probability of states of the atom. In addition, we simulate the momentum change of the atom due to the spontaneous emission of light by the atom and due to absorption and stimulated emission fluctuations, which also results in the to atomic momentum fluctuations. In our calculations, for simplicity, we assume that the spontaneous emission of a photon by an atom leads to the change $\hbar k$ in the atom's momentum with the same probability in the positive and negative directions of the axes Ox and Oy .

The stochastic nature of the spontaneous emission of light by an atom causes the atom's diffusion in the momentum space, the so-called "momentum diffusion". In the field of low-intensity laser radiation, when the population of the excited state is insignificant, the light pressure force and the momentum diffusion coefficient are equal to the sum of the corresponding quantities for each of the counter-propagating waves [28]. We used this approximation earlier to simulate the momentum diffusion in the field of counter-propagating light pulses of low intensity [18], as well as for estimation of momentum diffusion in the field of bichromatic [19], stochastic [20, 29] and frequency-modulated [21] light waves.

We simulate the change in the atomic momentum due to the recoil effect of the spontaneous emission by modeling the direction of the photon propagation. For example, we may divide the interval from 0 to 1 into four identical intervals, each of which corresponds to the radiation of a photon along the positive or negative axes direction Ox , Oy and check, if the uniformly distributed between 0 and 1 random variable gets into one of four intervals.

Calculation of the momentum fluctuation due to the absorption and stimulated emission fluctuations requires additional attention. Let's consider the atomic momentum fluctuations in the field of a travelling monochromatic waves. Let θ be the angle between the direction of the spontaneously emitted photon and axis Ox , along which the light wave propagates, $\langle N_s \rangle$ is the average number of spontaneously emitted photons. Then, assuming the scattering of the photons to be completely random process, we have for the average square of the momentum change of the ensemble of atoms [25]:

$$\langle \Delta p_x^2 \rangle = \langle \Delta p_{0x}^2 \rangle + \hbar^2 k^2 \langle N_s \rangle + \hbar^2 k^2 \langle \cos^2 \theta \rangle \langle N_s \rangle. \quad (45)$$

The first term on the right hand side of (45) is the initial moment distribution of the atoms, the second is due to the stimulated processes (absorption and emission), the third term is due to the fluctuations of the momentum in the spontaneous emission of photons. This equation is the basis for the computer simulation of the momentum diffusion in the field of one travelling wave. According to (45), for each random change of the atomic momentum due to the spontaneous emission of light, one change in the atomic momentum at $\pm \hbar k$ occurs due to the stimulated processes. This algorithm for calculating momentum diffusion of atoms is valid for a weak field $\Omega_0 \lesssim \gamma$. If the intensity of the counter-propagating waves is large, we will take into account the momentum diffusion due to stimulated processes in the same way, knowing that the results we have obtained is the approximation to the strict consideration. Since we suppose the motion of atoms for the same intensity of criss-cross waves, one should expect that the fluctuation change of the square of x and the y -components of the momentum of the atoms due to stimulated processes are the same for averaging after several modulation periods.

After each step Δt of the integration of the equations (24), (40) and (41) we check if a quantum jump occurred during it and normalize the state vector. If the quantum jump occurred, the atom's velocity along the Ox axis varies by

$$\Delta v_x = \hbar k \operatorname{sgn}(\epsilon_1 - 0.5) \frac{1 + \operatorname{sgn}(\epsilon_2 - 0.5)}{2m} + \hbar k \operatorname{sgn}(\epsilon_3 - 0.5) \frac{1 + \operatorname{sgn}(\epsilon_4 - 0.5)}{2m}, \quad (46)$$

$$\Delta v_y = \hbar k \operatorname{sgn}(\epsilon_1 - 0.5) \frac{1 - \operatorname{sgn}(\epsilon_2 - 0.5)}{2m} + \hbar k \operatorname{sgn}(\epsilon_3 - 0.5) \frac{1 - \operatorname{sgn}(\epsilon_4 - 0.5)}{2m}, \quad (47)$$

where $\epsilon_{1,2,3,4}$ are the random numbers that are uniformly distributed in the interval $[0, 1]$. Here two terms simulate the fluctuation of the momentum with the spontaneous emission of the photon along the positive and negative directions of each of the axes; another two simulate the fluctuation of the momentum in the same directions due to the fluctuation of the stimulated absorption and emission processes.

VI. RESULTS OF THE NUMERICAL SIMULATUON

The time evolution of an atomic ensemble in a bichromatic field is determined by the parameters of the interaction of atoms with the field and the initial conditions. To simplify the analysis, we do not take into account the influence of the initial atomic distribution function of the coordinates and velocity components. We assume that the atoms begin to move from the same point, which is the origin of the coordinates ($x_0 = 0$, $y_0 = 0$), with the same velocity. We carried out our calculations for the atom ^{23}Na , for which a cyclic interaction with the field can be organized [1]. The wavelength of the transition

$3^2S_{1/2} - 3^2P_{3/2}$ is $\lambda = 589.16$ nm, the spontaneous emission rate $\gamma = 2\pi \times 10$ MHz, the Doppler cooling limit for sodium atoms is $T_D = 240 \mu\text{K}$ [1]. Similar calculations for the case of one standing bichromatic wave were carried out earlier in the paper [19]. We consider the motion of atoms in the case of criss-cross bichromatic waves for parameters similar to those used for numerical simulation in the paper [19], focusing on those that correspond to the formation of traps for atoms and the formation of periodic structures. In our case, obviously, one should expect the formation of a two-dimensional trap and two-dimensional spatial structures.

To check the possibility of forming a two-dimensional trap by the field of criss-cross bichromatic waves, the time dependences of the center of mass (mean values of abscissa and ordinates, x_{av} and y_{av}) of the ensemble of atoms and the root-mean-square deviation from the mean values Δx , Δy were calculated. An example of these dependencies is shown in Fig. 2. We do not present here the corresponding time dependencies of ordinates; they are

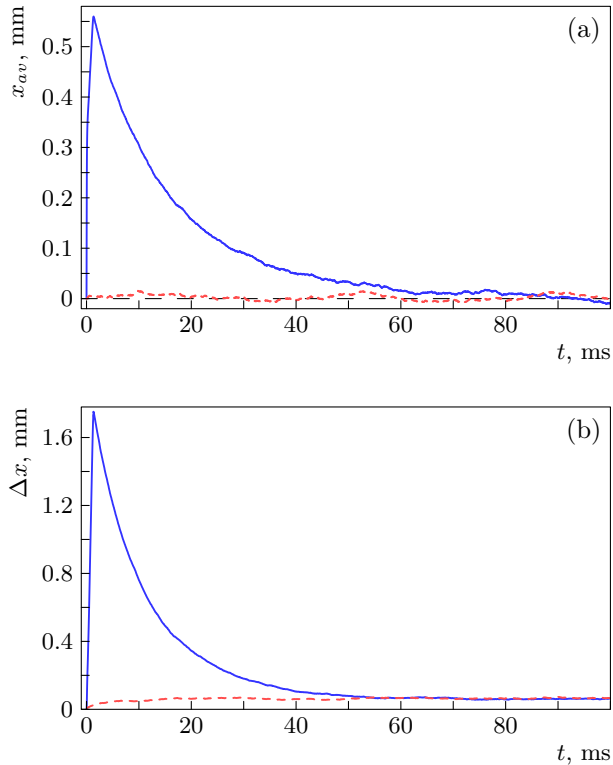


FIG. 2. The time dependence of the mean coordinate x_{av} (a) and the root mean square deviation Δx (b) of 100 ^{23}Na atoms under their interaction with criss-cross standing bichromatic waves. The components of the initial velocity of atoms are $v_{0x} = v_{y0} = 5$ m/s (solid curve), $v_{0x} = v_{y0} = 0$ (dashed curve), $\Omega = 200$ MHz, $\delta = 2\pi \times 20$ MHz ($\delta_1 = \delta_2 = \delta_5 = \delta_6 = 2\pi \times 110$ MHz, $\delta_3 = \delta_4 = \delta_7 = \delta_8 = -2\pi \times 90$ MHz), the Rabi frequencies are the same and equal to $\Omega_0 = 2\pi \times 100$ MHz, the initial phases of the waves equal to zero. Before the interaction with the field the atoms occupy the ground state.

similar to the corresponding dependences of x_{av} and Δx . As we see, in the case of the initial velocity of the atoms $v_{0x} = v_0 = 5$ m/s, when atoms move from the origin of coordinates, they are subjected to the light pressure force in the direction to the point $x = 0, y = 0$. Subsequently, the value x_{av} fluctuates near $x = 0$ (the same applies to y_{av}), and Δx and

Δy fluctuates near $\Delta x \approx 66 \mu\text{m}$. For greater certainty that approximately the stationary value is achieved, we carried out the similar calculations for zero initial velocity. The result was the same (see dashed curve in Fig. 2). This is a little more than a similar result for the one-dimensional trap $\Delta x \approx 50 \mu\text{m}$ (see Fig. 8 in paper [19]). We should note that in order to have a coordinate-dependent light pressure force directed towards the coordinates origin, the intensity of the light waves should be quite large [19].

Now we consider the formation of spatial structures of atoms by the field of the criss-cross standing bichromatic waves. We remind that the field of a standing bichromatic wave can form a one-dimensional grating of atoms with their grouping in planes at distances $\frac{1}{4}\lambda + \frac{1}{2}n\lambda$ from the origin of coordinates, where n is an arbitrary integer [19]. Fig. 3 depicts a fragment of the spatial distribution of ^{23}Na atoms after $100 \mu\text{s}$ of their interaction with the criss-cross stationary bichromatic waves. During this time, the stationary value of the components of

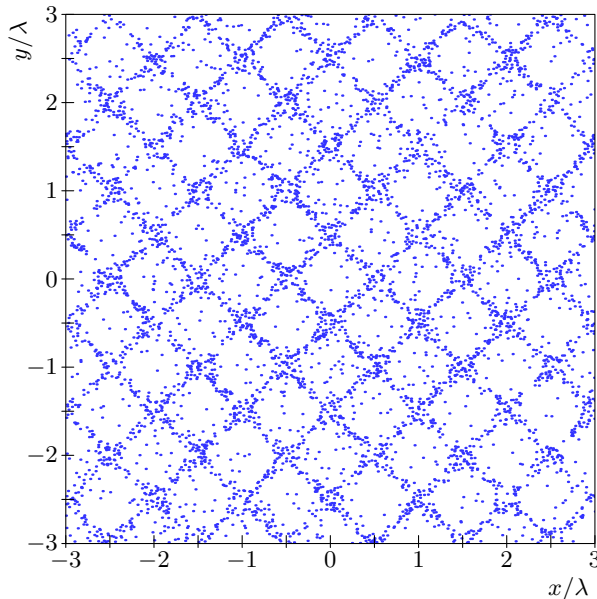


FIG. 3. A fragment of the spatial distribution of 50,000 ^{23}Na atoms after $100 \mu\text{s}$ of the interaction with the criss-cross standing bichromatic waves. The initial velocity of the atoms is zero, $\Omega = 2\pi \times 40 \text{ MHz}$, $\delta = 2\pi \times 20 \text{ MHz}$ ($\delta_1 = \delta_2 = \delta_5 = \delta_6 = 2\pi \times 120 \text{ MHz}$, $\delta_3 = \delta_4 = \delta_7 = \delta_8 = -2\pi \times 80 \text{ MHz}$), the Rabi frequencies of the waves are the same and equal to $\Omega_0 = 2\pi \times 100 \text{ MHz}$, the initial phases of all waves are equal to zero.

the root mean square deviation of the atoms velocity from the average value $\Delta v_x = \Delta v_y = 0.248 \text{ m/s}$ is established. For $t = 100 \mu\text{s}$, the root mean square deviation of the atoms coordinates from the mean value is $\Delta x \approx \Delta y \approx 4.5 \mu\text{m}$ and continues to grow.

The spatial distribution of atoms depicted in Fig. 3 is related to the spatial distribution of the the density of the energy of the electric field, averaged over time, which in this case is described by the expression

$$w = 8\varepsilon_0 E_0^2 [\sin^2(\pi x/\lambda) + \sin^2(\pi y/\lambda) - 1]^2. \quad (48)$$

Here we have taken into account that we are considering the distances of atoms from the origin of the coordinates, for which $x\Delta k \ll 1$, $y\Delta k \ll 1$. From the expression (48) it is easy

to see that the energy density is zero along the families of straight lines described by the equations

$$y = x + \frac{\lambda}{2} + n_1\lambda, \quad (49)$$

$$y = -x + \frac{\lambda}{2} + n_2\lambda, \quad (50)$$

where n_1, n_2 are integers. As shown in Fig. 3, most of the atoms are near the straight lines described by the equations (49), (50), that is, at points with low density of energy of the electric field. The explanation for such a phenomenon is quite simple. If the atom, while moving in the weak field, moves almost along the straight lines (49), (50), the direction of it's velocity changes with a very small probability, or changes after reaching the points with strong field. If the atoms pass through the region of a strong field, the probability of changing the direction of their velocity is much higher. Thus, in the distribution of velocities for atoms, we have a maximum near the directions corresponding to the motion of atoms along the straight lines (49), (50), which explains the formation of the spatial grating shown in Fig. 3. Figure 4 shows the trajectory of one of the atoms. It is well visible that a large part

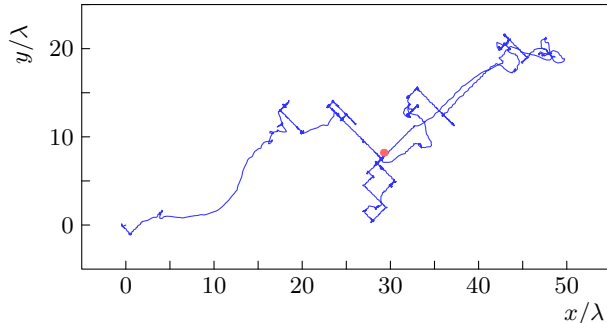


FIG. 4. Trajectory of the motion of one of the atoms for the parameters corresponding to Fig. 3. Time of motion is $500 \mu\text{s}$. The red circle shows the point corresponding to time $500 \mu\text{s}$

of the trajectory consists of segments directed at the angle $\pm\frac{1}{4}\pi$ to the axis of abscissa and ordinate in accordance with the equations (49), (50). Consequently, the two-dimensional grating of atoms in Fig. 3 has a dynamic character. The atoms move most of the time close to directions of the straight lines, defined by the equations (49) and (50), from time moving from one straight line to another. Figure 5 illustrates the distribution of the energy density of the electric field for the cases $\varphi = 0$ (a) and $\varphi = \pi$ (b). It is seen that energy is mainly concentrated near the points $x = n_x\lambda, y = n_y\lambda$ (a), where n_x, n_y are arbitrary integers, and near the points $x = n_x\lambda + \frac{1}{2}\lambda, y = n_y\lambda + \frac{1}{2}\lambda$ (b). The structure formed by atoms for $\varphi = 0$ (Fig. 3) corresponds to the regions of the weak field in Fig. 5a. If $\varphi = \pi$, the areas of the strong field are shifted by $\lambda/2$ along the axis of abscissas and ordinates in comparison with the case $\varphi = 0$; we see again that most of the atoms are in the region of a weak field (see Fig. 6). Contrary to Fig. 3, in Fig. 6 there is a noticeable difference in the density of atoms in the center of the figure and at its periphery. This is due to the slower expansion of the cloud of atoms, since the field is very small near the initial coordinates ($x_0 = 0, y_0 = 0$) for $\varphi = \pi$. As the result there is a smaller characteristic dimension of the atomic cloud ($\Delta x = \Delta y = 2.5 \mu\text{m}$ versus $\Delta x = \Delta y = 4.5 \mu\text{m}$ for $\varphi = 0$).

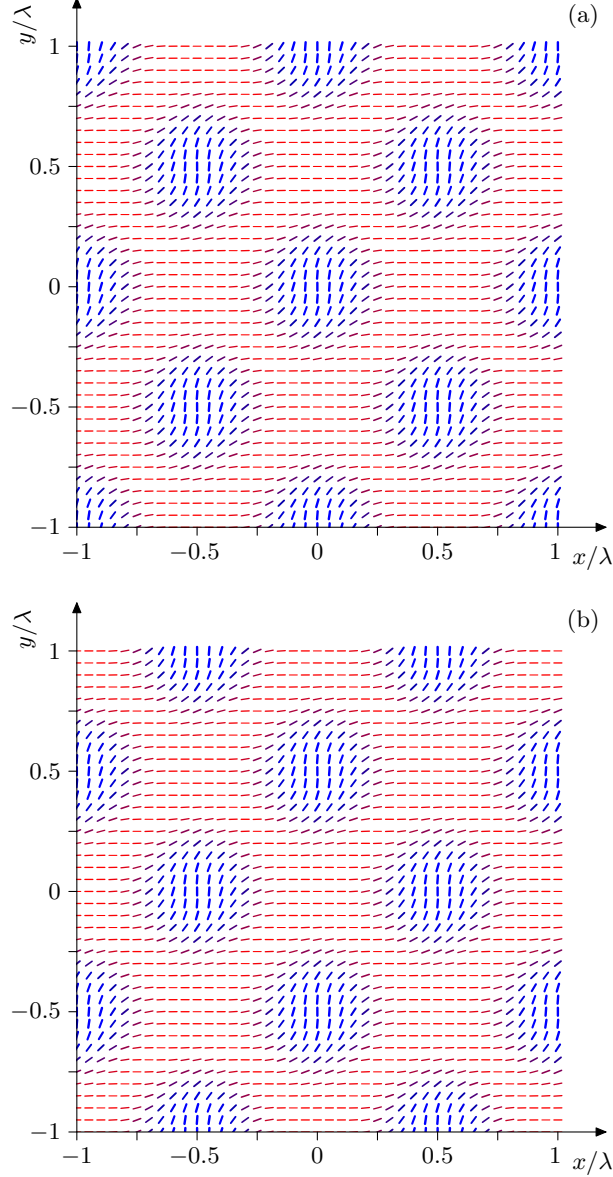


FIG. 5. The distribution of the energy density of the electric field of the criss-cross standing bichromatic waves for cases $\varphi = 0$ (a), when the phases of all waves are the same, and $\varphi = \pi$ (b), when the phases of the waves propagating along the ordinate axis differ on $\varphi = \pi$ from the phases of the waves propagating along the abscissa axis. The angle of inclination of the strokes to the abscissa axis is proportional to the energy density of the field.

Note that in the general case of the arbitrary values of the phase shift φ between the criss-cross waves, generally speaking, there are no such lines in space, for which the density of the electric field energy, averaged over time,

$$\begin{aligned}
 w = 4\varepsilon_0 E_0^2 & \left[2 \left(\sin^2(\pi x/\lambda) + \sin^2(\pi y/\lambda) \right)^2 + \right. \\
 & + 4(\cos \varphi - 1) \sin^2(\pi x/\lambda) \sin^2(\pi y/\lambda) + \\
 & + \left(1 - 2 \sin^2(\pi x/\lambda) - 2 \sin^2(\pi y/\lambda) \right) \times \\
 & \left. \times (1 + \cos \varphi) \right], \tag{51}
 \end{aligned}$$

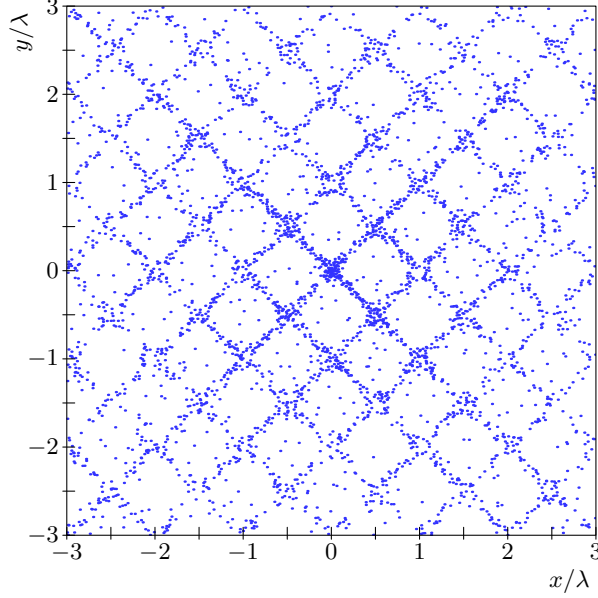


FIG. 6. A fragment of the spatial distribution of 50,000 atoms ^{23}Na after 100μ of interaction with the criss-cross standing bichromatic waves. The initial velocity of atoms is zero, $\Omega = 2\pi \times 40$ MHz, $\delta = 2\pi \times 20$ MHz ($\delta_1 = \delta_2 = \delta_5 = \delta_6 = 2\pi \times 120$ MHz, $\delta_3 = \delta_4 = \delta_7 = \delta_8 = -2\pi \times 80$ MHz), the Rabi frequencies of the waves are the same and equal to $\Omega_0 = 2\pi \times 100$ MHz, $\varphi_1 = \varphi_2 = \varphi_3 = \varphi_4 = 0$, $\varphi_5 = \varphi_6 = \varphi_7 = \varphi_8 = \pi$.

would be zero. For example, for $\varphi = \pi/2$ the equation (51) leads to the expression

$$w = 4\varepsilon_0 E_0^2 [\sin^2(\pi x/\lambda) + \sin^2(\pi y/\lambda) - 1]^2 + \sin^4(\pi x/\lambda) + \sin^4(\pi y/\lambda), \quad (52)$$

which at any point is not zero. At the same time there may be rectilinear regions with a rather low energy density, which makes it possible to form spatial gratings. In particular, the results, which are close to the results shown in Fig. 3 and 6, are observed at small changes in the phase shift between the criss-cross waves, respectively, at $\varphi = 0.05\pi$ and $\varphi = 0.95\pi$.

The spatial structures of the clouds of atoms in the fields of the criss-cross standing bichromatic waves arise due to the joint action of both waves on the atom and can not be interpreted by generalizing the results of the study of spatial structures of atoms in the field of a standing bichromatic wave [19] to a two-dimensional case. Indeed, in one standing bichromatic wave, atoms are grouped in planes with $x = \frac{1}{4}\lambda + \frac{1}{2}n\lambda$ (n is an integer) for waves propagating along the abscissa axis and $y = \frac{1}{4}\lambda + \frac{1}{2}n\lambda$ for waves propagating along the ordinate axis.

Extrapolating these results in a two-dimensional case, one would expect the grouping of atoms near the points with coordinates $x = \frac{1}{4}\lambda + \frac{1}{2}n_x\lambda$, $y = \frac{1}{4}\lambda + \frac{1}{2}n_y\lambda$, which does not correspond to the results obtained in this paper, namely, a spatial grating with the period $\frac{\sqrt{2}}{2}\lambda$, oriented at an angle $\pi/4$ to the abscissa and ordinate axes.

VII. CONCLUSIONS

We investigated the spatial distribution of atoms in the field of criss-cross bichromatic standing waves. As it turned out, using the previous study of the spatial distribution of atoms in the field of a standing bichromatic wave [19], we can estimate the parameters and character of the distribution of atoms in the field of criss-cross standing bichromatic waves only partially. Thus, the parameters of the distribution of atoms in the light trap created by such fields are in good agreement with the parameters expected on the basis of paper [19]. At the same time, the appearance of the spatial structure can not even be approximated by extrapolating the results of the paper [19] for a one-dimensional case on a two-dimensional case; instead of the expected grouping of atoms near the points $x = \frac{1}{4}\lambda + \frac{1}{2}n_x\lambda$, $y = \frac{1}{4}\lambda + \frac{1}{2}n_y\lambda$, where n_x, n_y — arbitrary integers, the atoms group in a neighborhood of lines that correspond to the minimum energy. As a result, the cloud of atoms form a grid with the side equal to $\frac{\sqrt{2}}{2}\lambda$. This grating has a dynamic character. The atoms, that are part of it, spend some, relatively short, time there, moving along its sides, then exit and after some time enter another place of the grating.

ACKNOWLEDGMENTS

The publication is based on the research supported by the goal-oriented complex program of fundamental researches of the National Academy of Sciences of Ukraine “Fundamental issues in creation of new nanomaterials and nanotechnologies” (grant No. 3/18-H).

-
- [1] H. J. Metcalf and P. van der Stratten. *Laser Cooling and Trapping*. Springer-Verlag: New York, Berlin, Heidelberg, 1999.
 - [2] A. M. Negriyko, V. I. Romanenko, and L. P. Yatsenko. *Dynamics of atoms and molecules in coherent laser fields (in Ukrainian)*. Naukova dumka: Kyiv, 2008.
 - [3] Harold Metcalf. Colloquium: Strong optical forces on atoms in multifrequency light. *Rev. Mod. Phys.*, 89:041001, Oct 2017.
 - [4] V. S. Voitsekhovich, M. V. Danileiko, A. N. Negriiko, V. I. Romanenko, and L.P. Yatsenko. Light pressure on atoms in counterpropagating amplitude-modulated waves. *Zhurnal Tekhnicheskoi Fiziki*, 58:1174–1176, 1988.
 - [5] A. P. Kazantsev and I. V. Krasnov. Rectification effect of a radiation force. *J. Opt. Soc. Am. B*, 6(11):2140–2148, Nov 1989.
 - [6] V. S. Voitsekhovich, M. V. Danileiko, A. N. Negriiko, V. I. Romanenko, and L.P. Yatsenko. Observation of a stimulated radiation pressure of amplitude-modulated light on atoms. *JETP Lett.*, 49:161–164, Nov 1989.
 - [7] R. Grimm, Yu. B. Ovchinnikov, A. I. Sidorov, and V. S. Letokhov. Observation of a strong rectified dipole force in a bichromatic standing light wave. *Phys. Rev. Lett.*, 65:1415–1418, Sep 1990.
 - [8] Yu B Ovchinnikov, R Grimm, AI Sidorov, and VS Letokhov. Rectified dipole force in a bichromatic standing light wave. *Optics communications*, 102(1-2):155–165, 1993.

- [9] J. Söding, R. Grimm, Yu. B. Ovchinnikov, Ph. Bouyer, and Ch. Salomon. Short-distance atomic beam deceleration with a stimulated light force. *Phys. Rev. Lett.*, 78:1420–1423, Feb 1997.
- [10] M. R. Williams, F. Chi, M. T. Cashen, and H. Metcalf. Bichromatic force measurements using atomic beam deflections. *Phys. Rev. A*, 61:023408, Jan 2000.
- [11] M. T. Cashen and H. Metcalf. Bichromatic force on helium. *Phys. Rev. A*, 63:025406, Jan 2001.
- [12] Christopher Corder, Brian Arnold, and Harold Metcalf. Laser cooling without spontaneous emission. *Phys. Rev. Lett.*, 114:043002, Jan 2015.
- [13] Christopher Corder, Brian Arnold, Xiang Hua, and Harold Metcalf. Laser cooling without spontaneous emission using the bichromatic force. *J. Opt. Soc. Am. B*, 32(5):B75–B83, May 2015.
- [14] Harold Metcalf. Entropy exchange in laser cooling. *Phys. Rev. A*, 77:061401, Jun 2008.
- [15] T. G. M. Freegarde, J. Waltz, and W. Hänsch. Confinement and manipulation of atoms using short laser pulses. *Opt. Commun.*, 117:262–267, 1995.
- [16] A. Goepfert, I. Bloch, D. Haubrich, F. Lison, R. Schütze, R. Wynands, and D. Meschede. Stimulated focusing and deflection of an atomic beam using picosecond laser pulses. *Phys. Rev. A*, 56:R3354–R3357, 1997.
- [17] V. I. Romanenko and L. P. Yatsenko. Theory of one-dimensional trapping of atoms by counterpropagating short pulse trains. *J. Phys. B*, 44:115305, 2011.
- [18] V. I. Romanenko, Ye. G. Udovitskaya, A. V. Romanenko, and L. P. Yatsenko. Cooling and trapping of atoms and molecules by counterpropagating pulse trains. *Phys. Rev. A*, 90:053421, Nov 2014, arXiv:1408.5074 [physics.atom-ph].
- [19] V. I. Romanenko, A. V. Romanenko, and L. P. Yatsenko. An optical trap for atoms on the basis of counter-propagating bichromatic light waves. *Ukr. J. Phys.*, 61:309–324, 2016.
- [20] V. I. Romanenko and L. P. Yatsenko. Trapping of atoms by the counter-propagating stochastic light waves. *Optics Communications*, 392:239 – 246, 2017, arXiv:1610.01831v2 [physics.atom-ph].
- [21] Victor I Romanenko and Nataliya V Kornilovska. Atoms in the counter-propagating frequency-modulated waves: splitting, cooling, confinement. *The European Physical Journal D*, 71(9):229, 2017.
- [22] C. Mølmer, Y. Castin, and J. Dalibard. Monte carlo wave-function method in quantum optics. *J. Opt. Soc. Am. B*, 10:524–538, 1993.
- [23] Leonid Yatsenko and Harold Metcalf. Dressed-atom description of the bichromatic force. *Physical Review A*, 70(6):063402, 2004.
- [24] A. P. Kazantsev. Acceleration of atoms by light. *Zh. Éksp. Teor. Fiz.*, 66:1599–1612, 1974.
- [25] V. G. Minogin and V. S. Letokhov. *Laser Light Pressure on Atoms*. Gordon and Breach: New York, 1987.
- [26] J. Steinbach, B. M. Garraway, and P. L. Knight. High-order unraveling of master equations for dissipative evolution. *Phys. Rev. A*, 51:3302–3308, Apr 1995.
- [27] B. W. Shore. *The Theory of Coherent Atomic Excitation, Vol. 1*. Wiley: New York, 1990.
- [28] Klaus Mølmer. Limits of doppler cooling in pulsed laser fields. *Phys. Rev. Lett.*, 66:2301–2304, May 1991.
- [29] V. I. Romanenko, O. G. Udovytska, V. M. Khodakovsky, and L. P. Yatsenko. Atomic momentum diffusion in the field of counter-propagating stochastic light waves. *Ukr. J. Phys.*, 63:616–622, 2018.